Effect of *trans*- and *cis*-Isomeric Defects on the Localization of the Charged Excitations in π-Conjugated Organic Polymers

Iffat H. Nayyar,[1,2,3] Enrique R. Batista,[1] Sergei Tretiak,[1,4] Avadh Saxena,[1] Darryl L. Smith,[1] Richard L. Martin[1]

[1]Theoretical Division and Center for Nonlinear Studies, Los Alamos National Laboratory, Los Alamos, New Mexico 87545
[2]NanoScience Technology Center, University of Central Florida, Orlando, Florida 32826
[3]Department of Physics, University of Central Florida, Orlando, Florida 32826
[4]Center for Integrated Nanotechnologies, Los Alamos National Laboratory, Los Alamos, New Mexico 87545
Correspondence to: S. Tretiak (E-mail: serg@lanl.gov)

Received 12 March 2013; accepted 13 March 2013; published online 9 April 2013
DOI: 10.1002/polb.23291

ABSTRACT: We use the long-range-corrected hybrid density functional theory models to study the effect of various conformational distortions of weak-*trans* and strong-*cis* nature on the spatial localization of charged states in poly(*p*-phenylene vinylene) (PPV) and its derivative poly[2-methoxy-5-(2′-ethylhexyloxy)-*p*-phenylene vinylene] (MEH-PPV). The extent of self-trapping of positive (P^+) and negative (P^-) polarons is observed to be highly sensitive to molecular conformation that, in turn, controls the distribution of atomic charges within the polymers. It is shown that, to reach good agreement with recent experimental data on lattice distortion for P^+ and P^- excitations, the polarization of the medium plays a critical role. The introduction of weak-*trans* defects along the MEH-PPV chain breaks the observed symmetry for P^+ and P^- excitations. The P^- states exhibit more spatial localization owing to lattice relaxation than their vacuum counterparts in contrast to P^+. These observations suggest higher mobilities of holes than that of electrons in MEH-PPV, in agreement with the experimental observations. The predicted binding, reorganization, and solvation energies for PPV and MEH-PPV are analyzed for this difference in the response behavior of holes and electrons for *trans* and *cis* distortions. This study allows for a better understanding of charge-transport and photophysical properties in π-conjugated organic materials by analyzing their underlying structure–property correlations. © 2013 Wiley Periodicals, Inc.† J. Polym. Sci., Part B: Polym. Phys. **2013**, *51*, 935–942

KEYWORDS: conducting polymers; conjugated polymers; quantum chemistry; theory; UV-vis spectroscopy

INTRODUCTION Organic π-conjugated polymers form an important class of optoelectronic materials[1] with a variety of applications in light-emitting diodes,[2,3] field-effect transistors,[4,5] and solar cells.[6–8] The performance of these devices is determined by the charge carrier energetics and transport properties between the donor and the acceptor molecules in semiconducting polymer materials.[9–13] For instance, the oppositely charged carriers (holes and electrons) form the weakly bound neutral pairs in a light-emitting diode if the Coulombic attraction between them exceeds their thermal energy. These pairs then dissociate radiatively or nonradiatively to form singlet or triplet neutral excitons, giving rise to the device electroluminescence or electrophosphorescence, respectively.[3,14,15] On the other hand, the light absorption in a photovoltaic cell results in the formation of the neutral excited states at the heterojunctions which then dissociate into the photo-generated holes and electrons producing the photocurrent.[16–19] Thus, the detailed understanding of the nature and dynamics of these primary neutral and charged excitations (excitons and polarons), their propagation along and among the chains and the interaction between the excited electronic states is critical in improving the efficiency of these electro-optical devices.[20–25] Among several types of conjugated polymers, poly(*p*-phenylene vinylene) (PPV) and poly[2-methoxy-5-(2′-ethylhexyloxy)-*p*-phenylene vinylene] (MEH-PPV) are currently two of the most investigated systems because of their high luminescence efficiency, facile processing, electronic tunability, and a wide range of experimental evidence.[26–28] Furthermore, the extremely long spin coherence times owing to their weak intermolecular spin-orbit interaction of *van der* Waals type and small hyperfine field are favorable for studying the extension and migration of electrically or photo-generated neutral and charged states within these systems.[27,29]

Additional Supporting Information may be found in the online version of this article.

Earlier, we conducted a comprehensive density functional theory (DFT) and time-dependent DFT (TD-DFT) study[30,31] for neutral and charged self-localized excited states in PPV and MEH-PPV oligomers in their *trans* geometries without any torsional distortions along their backbones. The functionalization of PPV with alkoxy side chains was demonstrated to have a negligible effect on the spatial localization of the electronic excitations. Also, the particle-hole symmetry was preserved in the *trans*-isomeric form of the polymers. However, some of these observations for isolated perfect chains are found to be in contrast to the previous experimental[32] and theoretical[33] studies, observing the strong dependence of the response of the opposite carriers on the molecular structure and distribution of the atomic charges within the polymers. In molecular clusters, Yang et al.[34,35] observed an asymmetry in the behavior of hole and electron traps owing to the weaker intramolecular interactions between different conjugated segments of MEH-PPV than for unsubstituted PPV. Recently, an experimental study[27] revealed substantial difference in the optically detected magnetic resonance response by the opposite charges constituting a polaron pair for MEH-PPV organic light-emitting diodes. The asymmetry in the behavior of these charges was attributed to the different number of nuclear spins interacting with them, determining their degree of localization. Hence, the polymer traps the electron more tightly than the hole due to the self-trapping being inversely related to the extent of hyperfine field felt. The electron- and energy-transfer properties for the *trans* and *cis* isomers were also revealed to vary for oligo(phenylene vinylene) derivatives with various side-chain substitutions.[36,37] The fluorescence intensity of the optoelectronic devices was shown to improve by the introduction of *cis* defects into the backbone of the PPV derivatives.[38–40] Further, in a theoretical study,[41] the hole and electron-transport properties were observed to be markedly different for *cis* conformations of PPV derivatives in comparison to the *trans* ones.

These studies, focusing on the effect of the functionalization of the PPV polymer on the charge carrier-transport properties, motivated us to carry out our present investigation. In this contribution, we explore the effect of the presence of *trans* and *cis* types of conformational defects and alkoxy side groups on the localization of the charged excitations in PPV using DFT calculations. We are interested in describing the interactions between the oppositely charged carriers and the one-dimensional polymer chains owing to various conformational irregularities induced within them.

COMPUTATIONAL METHODOLOGY

We study the positive (P^+) and negative (P^-) polarons using the long-range-corrected LC-wPBE functional for ten-repeat-unit oligomers of PPV and MEH-PPV with different types of conformational defects along their length. Each repeat unit consists of a phenyl ring attached to a vinyl bridge. The importance of the inclusion of long-range corrections to the exchange for the description of these excitations in accordance with the experimental measurements was benchmarked in our previous contributions.[30,31,42–44] The defects of *trans* nature are introduced by applying a 180° rotation of the dihedral angle between phenyl and vinyl units, forming a weak bend along the length of the chain. Similarly, the *cis* defect is produced by a strong bend involving a 180° rotation of one of the vinyl bonds along the polymer. Henceforth, we refer to the "weak-*trans*" and "strong-*cis*" defects as the "small kink" (SK) and the "large kink" (LK), respectively. These kinks break the symmetry of the π-conjugation along the chain, dividing the chain into two distinct segments of equal or unequal length. Here, we study the effect on the localization of charged excitations owing to the introduction of structural defects of *trans* and *cis* nature in comparison to the undistorted *trans* geometry. The different geometrical configurations belonging to the same isomer type differ in their respective position of the kink on the chain. Figure 1 shows the scheme for all considered geometrical configurations in this study of MEH-PPV oligomers, namely, (a) *trans*, (b) *trans*-SK (6-3), (c) *trans*-SK (7-2), (d) *cis*-LK (4-4), and (e) *cis*-LK (5-3). The two numerals in the parenthesis denote the number of vinyl bonds on either side of the kink. Similar structures have been investigated for PPV oligomers as well.

All computations have been performed using the Guassian09 suite[45] and the 6–31G* basis set. In our calculation model, the alkoxy side-chain groups OC_8H_{17} were replaced by OCH_3 in MEH-PPV to speed up the numerical calculations. Past tests show that this is a valid approximation and it does not significantly affect the electronic structure of the backbone.[30,31] Optimal geometries of P^+ and P^- states were obtained using a standard self-consistent field scheme of cation and anion spin states, respectively. A moderately polar solvent, acetonitrile ($\varepsilon = 37.5$), is included via the conductor-like polarizable continuum model as implemented in Gaussian09 software package to mimic the polymer's highly polarizable dielectric environment in this study by matching its optical dielectric permittivity. Although this may be an overestimation of the static dielectric constant of PPV, but it is in good agreement with the polymer's large dynamic dielectric value. Additional calculations (data not shown) have revealed the same solvent-induced localization with a low-polarity solvent, tetrahydrofuran ($\varepsilon = 7.6$), in comparison to the higher polarity solvent (acetonitrile) in these polymers.

RESULTS AND DISCUSSION

Figure 2 shows the effect of various defects on the localization properties of P^+ and P^- excitations in MEH-PPV (right panel) in comparison to PPV (left panel). Only the calculations in the presence of a dielectric medium are shown. Plotted are the bond length alternations (BLAs) of vinyl bonds along the length of the chain. The BLA parameter is defined as the difference between C—C single and double bonds in the vinyl bridge and determines the degree of Peierls distortion in conjugated molecular chains.[46,47] It is observed to reach its minimum, signifying the self-trapping of P^+ and P^- polarons for both the polymers at the middle of the chain for their undistorted *trans* geometries (top panels, Fig. 2).

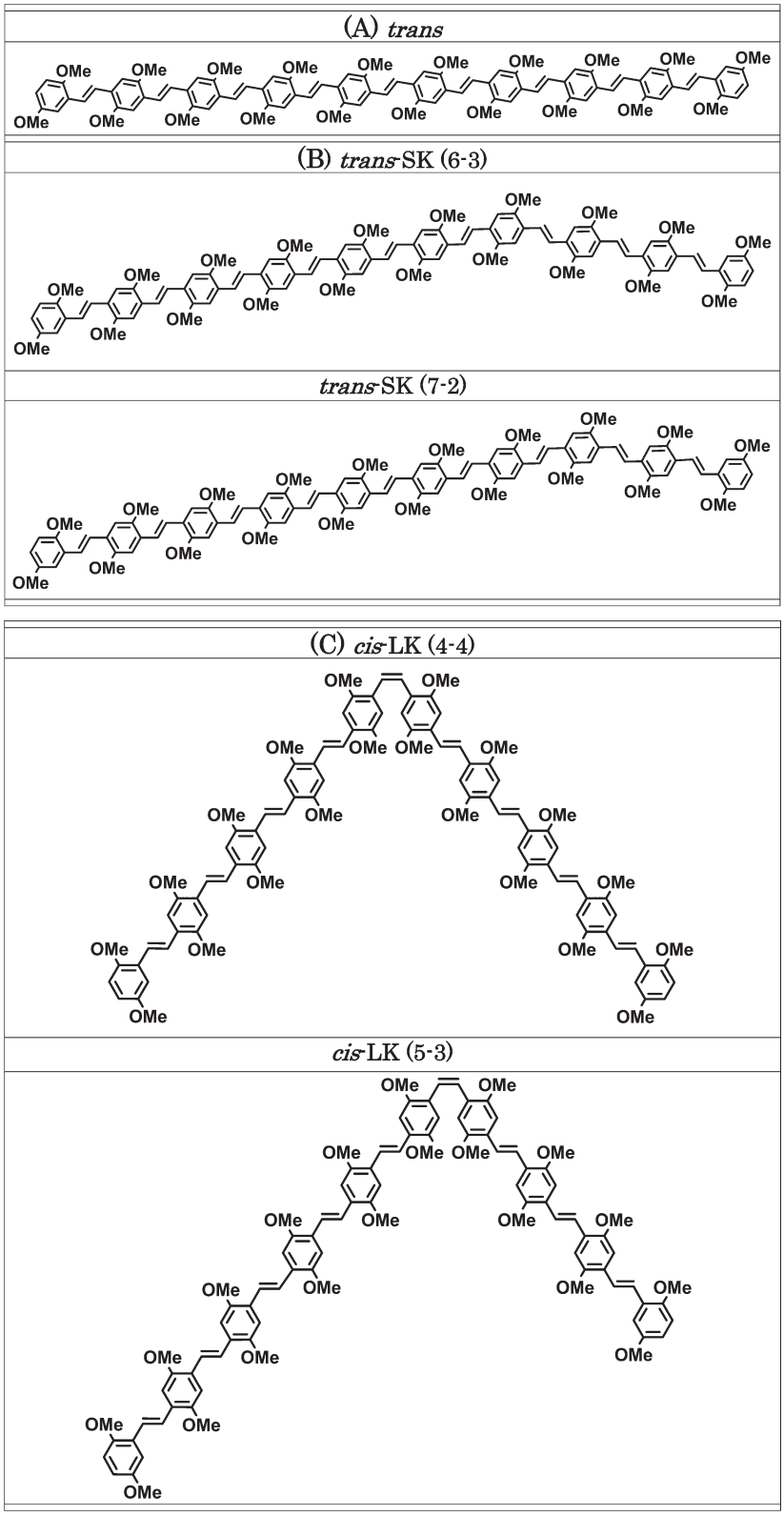

FIGURE 1 Studied geometrical configurations of MEH-PPV oligomer composed of 10 repeat units. (A) Undistorted *trans*-isomeric geometry. (B) Weak conformational defects (SKs) via a bend of *trans* form introduced at two different positions along the chain length. These defects are obtained by applying a 180° rotation of the dihedral angle between the phenyl and the vinyl units. (C) Strong conformational defects of *cis* nature (LKs) introduced at two different positions along the chain length. These defects are obtained by 180° rotation of one of the vinyl bonds. The left- and right-hand numerals in the parenthesis denote the number of vinyl bonds on either side of the kink.

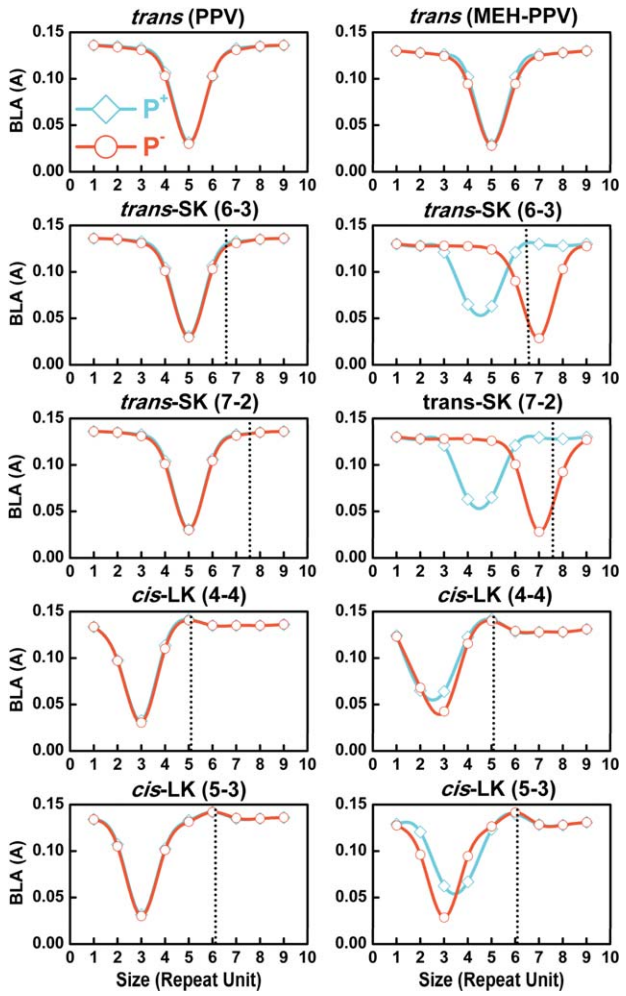

FIGURE 2 Variation of BLA (Å) for positive (P^+) and negative (P^-) polaronic excitations in PPV (left) and MEH-PPV (right) oligomers calculated at LC-wPBE/6–31G* level in the presence of solvent. The corresponding fully relaxed geometries are obtained for five different configurations: *trans*, *trans*-SK (6-3), *trans*-SK (7-2), *cis*-LK (4-4), and *cis*-LK (5-3). The dashed line represents the defect position on the chain.

However, PPV exhibits different localization patterns than MEH-PPV for various *trans* and *cis* defects as discussed below. The dashed line in the figure denotes the position of the defect along the chain length. The P^+ and P^- polarons continue to localize in the middle of the PPV chain with weak distortions of *trans* nature, whereas the observed particle-hole symmetry is completely broken for MEH-PPV chains, having the same nature of distortions. The P^- state now resides close to the defect position, whereas P^+ stays away from it. Interestingly, we observe the particle-hole symmetry to be roughly preserved for PPV and MEH-PPV oligomers having strong-*cis* distortions. In both these systems, the electrons and holes are repelled away from the *cis* defect site. The characteristic sizes of the P^+ and P^- excitations are found to be identical for PPV for all the considered configurations. This trend changes for MEH-PPV, where the size of the P^+ excitation is larger compared to that of P^- with the introduction of defects. The size is defined as the full width at half-maximum in terms of the repeat units of the BLA plots of the oligomer chains. Thus, we observe that the interaction of solvent with oligo(phenylene vinylene) chains is highly sensitive to their molecular geometry. The different behaviors of PPV and MEH-PPV are attributed to the presence of the alkoxy groups (OCH_3) on the phenyl rings in the latter, distributing a complex set of local dipoles along the molecular backbone. These trends are further shown in Supporting Information Figures 1S and 2S, plotting the BLAs and Mulliken atomic spin densities computed for P^+ and P^- states, respectively, of MEH-PPV oligomer in vacuum and solvent. Spin density distributions signify the spatial confinement of the electronic excitation owing to the polarization effects[30,31] playing an important role in the spatial confinement of positive polaron due to the trapping of electronic wavefunction, which ultimately results in the respective lattice distortions. Overall, the polarization of the medium increases the extent of both the structural and the electronic localization for negative polaron P^- unlike the trends observed for the positive polaron P^+.

The difference in the response of injected holes and electrons on MEH-PPV chains with weak-*trans* distortions intrigued us to further investigate these localization patterns as discussed below. We are interested in studying the behavior of holes (electrons) added to these systems in the native optimal geometries of P^- (P^+) states to understand whether the added holes (electrons) would still localize away from (close to) the weak-*trans*-defect sites and be able to overcome the energy barrier for hopping. The top and middle panels of Figure 3 demonstrate the BLA (left) and spin density (right) of P^+ (P^-) excitations on the MEH-PPV chains relaxed in the neutral ground (S_0) and charged P^- (P^+) states in the presence of solvent. Plotted are the *trans*-SK (6-3) (top) and *trans*-SK (7-2) (middle) configurations. In this figure, we have used a composite notation "(*X*,*Y*)" where *X* indicates the initial optimal state of the system before adding a charge carrier and *Y* denotes the final equilibrium state upon its addition. We observe that the system attains its equilibrium away from (close to) the defect upon P^+ (P^-) excitation from the uniform S_0 state. In contrast, it relaxes close to (away from) the defect when starting from the optimal P^- (P^+) state for P^+ (P^-) excitation. This suggests the existence of two energy minima for P^+ and P^- states for MEH-PPV geometries with weak-*trans* defects. The system at the global minimum of P^+ (P^-) state attains the local minimum configuration for P^- (P^+) with the addition of an electron (hole). For P^+, the two BLA minima for *trans*-SK (6-3) geometries differ by 13 meV (in energy) which is less than the average thermal fluctuations at room temperature (~25 meV), whereas they differ by 55 meV for P^- excitation. This also implies that the average drift mobility for the hole in these systems is higher than the electron, to be discussed in detail later in this section. Supporting Information Figure 3S shows a similar trend for the spin localization of the injected holes (electrons) into the weak *trans*-distorted systems

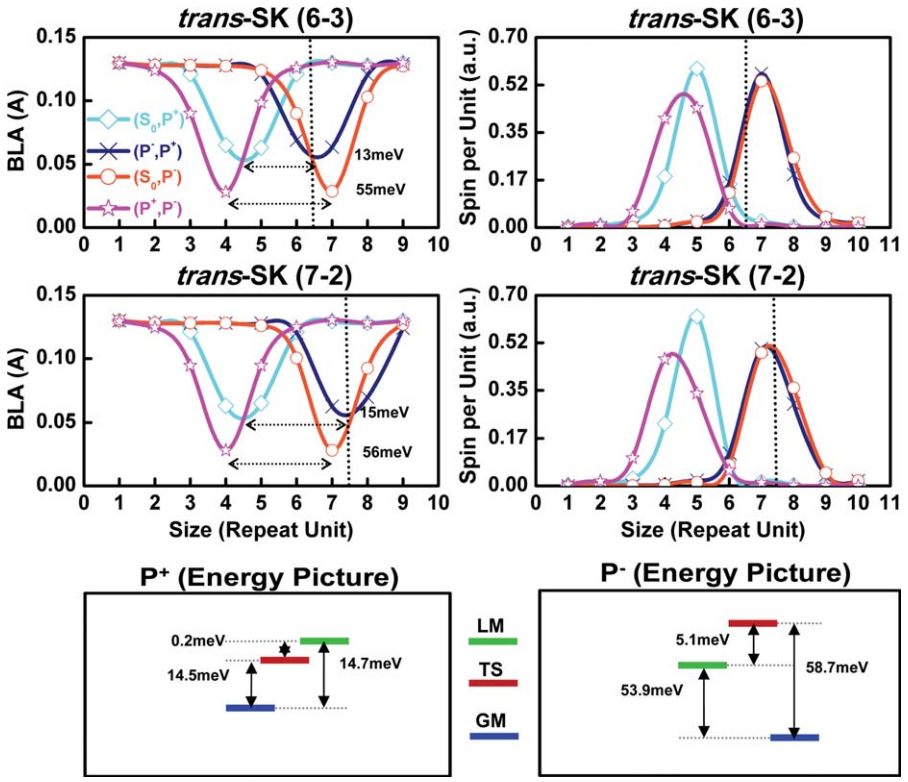

FIGURE 3 Variation of BLA (Å) (left) and Mulliken atomic spin densities (a.u.) per repeat unit (right) of the MEH-PPV oligomer in *trans*-SK (6-3) and *trans*-SK (7-2) geometrical configurations for positive (P^+) and negative (P^-) polarons. The calculations are performed at LC-wPBE/6–31G* level in the presence of a dielectric medium. We have used a notation "(*X*,*Y*)" in the legend, where *X* denotes the initial optimal state of the system before adding a charge carrier, whereas *Y* denotes the final equilibrium state. The dashed line represents the defect position on the chain. The bottom panel sketches the respective energy picture.

optimized in P^- (P^+) states and establishes the generality of our observations.

Our hypothesis for the existence of double-well potential energies for P^+ and P^- states (Fig. 3) can be explored in-depth from an alternative perspective in Supporting Information Figure 4S. We observe that the system attains equilibrium at two specified (4th and 7th units) positions on the chain irrespective of the initial state of injected holes and electrons. The potential energy barriers between the two BLA minima (global and local) are predicted to be 14.7 meV for P^+ and 53.9 meV for P^-. These observations are in accordance with the results contained in Figure 3 and validate the double-well energy potential surfaces for the charged species for *trans*-SK MEH-PPV geometries. The bottom panels of Figure 3 sketch the energy diagram for the two final optimal states attained for P^+ and P^- excitations along with their corresponding transition states. The transition states are lower by 0.2 meV for P^+ and higher by 5.1 meV for P^- from their corresponding local minima. This indicates a potential for deeper negative polaron trapping in MEH-PPV materials.

We further analyze trends in the excitation reorganization energies (Table 1) owing to geometry relaxation and solvation energies (Table 2). The reorganization energy is defined as the sum of two geometry relaxation energies: one is the binding energy and the other is the total energy of the neutral (S_0) state in the charged-state geometry (X) and that in S_0 geometry for organic crystals. Binding energy is an important parameter controlling the charge transport in conjugated polymers[48,49] and is summarized in Supporting Information Table 1S. We observe that the geometry relaxation effects in the presence of a polar solvent are much more pronounced in PPV than for MEH-PPV. The binding energies for P^+ states are tabulated to be smaller in magnitude than those for P^-. This difference is much more pronounced for the *trans* distortions upon addition of a solvent. The reorganization energy signifies the geometrical change in conjugated polymers upon excitation by a charge carrier.[41] According to the Marcus hopping model,[50] the reorganization energies are inversely proportional to the charge carrier hopping rates, determining their transport properties in π-conjugated systems. All distorted geometry types (*trans*-SK and *cis*-LK defects) considered in this study are observed to show similar hole- and electron-transport properties for PPV in solvent, unlike those observed for MEH-PPV. The *trans*- and *cis*-distorted geometries exhibit higher hole transport (lower reorganization energies) than electron transport for MEH-PPV. Inclusion of a polarizable medium provides a much higher stabilization for the P^+ states for distorted *trans* and *cis* geometries than for P^- states observed in MEH-PPV oligomers. This is attributed to the different

TABLE 1 Reorganization Energies (eV) for P^+ and P^- Polarons Calculated for All the Five Geometrical Conformations Under Study for Both Oligomers[a]

System	PPV				MEH-PPV			
Excitation (X)	P^+		P^-		P^+		P^-	
Medium	*V*	*S*	*V*	*S*	*V*	*S*	*V*	*S*
Conformation	Reorganization energy [binding energy + $\{E(X,S_0) - E(S_0,S_0)\}$] (eV)							
trans	0.75	0.57	0.79	0.60	0.62	0.53	0.65	0.58
trans-SK (6-3)	0.73	0.58	0.78	0.62	0.61	0.47	0.70	0.63
trans-SK (7-2)	0.74	0.58	0.78	0.62	0.62	0.47	0.70	0.63
cis-LK (4-4)	0.94	0.59	1.02	0.62	0.60	0.47	0.67	0.57
cis-LK (5-3)	0.76	0.59	0.80	0.63	0.62	0.47	0.65	0.57

The total energy of the S_0 state in the optimal geometry of the excitation (*X*) and that in its native geometry is added to the binding energies.

characteristic sizes (localization strengths) for the hole and electron for MEH-PPV geometries (Fig. 2). In addition, for *trans* defects the P^+ and P^- excitations are localized at two different positions on the MEH-PPV chain. Hence, the predicted reorganization energies are in close agreement with the trends observed for their corresponding localization strengths (Fig. 2). Supporting Information Figure 5S examines the density of single-particle states (Kohn–Sham orbitals) for P^+ and P^- excitations in their corresponding native states for the different geometry types considered in this study for MEH-PPV. The detailed description of these states for undistorted *trans* geometry has been provided in ref. 31. We do not observe any difference in the Kohn–Sham orbitals with the introduction of *trans* or *cis* defects into the system. However, the similar values of the binding and reorganization energies for each of these geometry types already suggest this.

Table 2 summarizes the solvation energies for P^+ and P^- states of PPV and MEH-PPV oligomers. This quantity is defined as the difference between the total energy of the charged excitation (*X*) in vacuum and that in the solvent, both calculated using the S_0 geometry. We observe that the geometry types do not have much influence on the solvation energies for either of the excitations for PPV and MEH-PPV. A polar solvent seems to provide a greater stabilization of about 0.8 eV to the P^- state in comparison to P^+ for MEH-PPV. The difference in the solvation energies for P^+ and P^- states in PPV is half of that computed for these states in MEH-PPV. The observed asymmetry in P^+ and P^- solvation energies is due to the difference in the distribution of local atomic charges within P^+ and P^- charged chains of PPV. The larger P^- energies are attributed to the ability of carbons to accommodate more partial negative charge in comparison to P^+. This leads to the higher stabilization of the C—H interactions for P^- excitations.[33] Finally, the P^- energy values are observed to further increase for MEH-PPV owing to the presence of the more electronegative oxygen atom.

Observed trends can be illustrated using the spatial distributions of molecular and natural orbitals. Figure 4 shows the characteristic highest occupied molecular orbital (HOMO) and lowest unoccupied molecular orbital (LUMO) orbitals for P^+ and P^- states in their corresponding native geometries for the *trans*-SK (6-3) geometry of MEH-PPV oligomer in the presence of solvent. The highest energy valence state belongs to the α-orbitals, whereas the lowest energy conduction state belongs to the β-orbitals. The β-LUMO of P^+ represents a localized state of a positive polaron, whereas the α-HOMO represents a polaronic state for the P^- excitation. We observe the P^- state to spread around the defect in contrast to the P^+ excitation. Orbital analysis of electronic excitations was conducted using the natural orbital (NO) representation for the singly occupied electronic levels which is also shown in Figure 4. The NOs are defined as the eigenfunctions of spinless one-particle electron density matrix. The P^+ and P^- states have only one NO with unit occupation localized away and on the defect, respectively.

TABLE 2 Solvation Energies (eV) of PPV and MEH-PPV Oligomers for P^+ and P^- Excitations for all Five Geometrical Conformations Under Study Calculated at LC-wPBE/6–31G* level[a]

System	PPV		MEH-PPV	
Excitation (*X*)	P^+	P^-	P^+	P^-
Conformation	Solvation energy ($E[S_0,X]_V - E[S_0,X]_S$) (eV)			
trans	2.13	2.38	2.52	3.37
trans-SK (6-3)	2.10	2.35	2.55	3.38
trans-SK (7-2)	2.09	2.34	2.57	3.37
cis-LK (4-4)	2.27	2.58	2.50	3.34
cis-LK (5-3)	2.08	2.34	2.55	3.32

The difference between the total energy of the excitation (*X*) in vacuum and that in the solvent is reported. Both energies are calculated in the S_0 geometry.

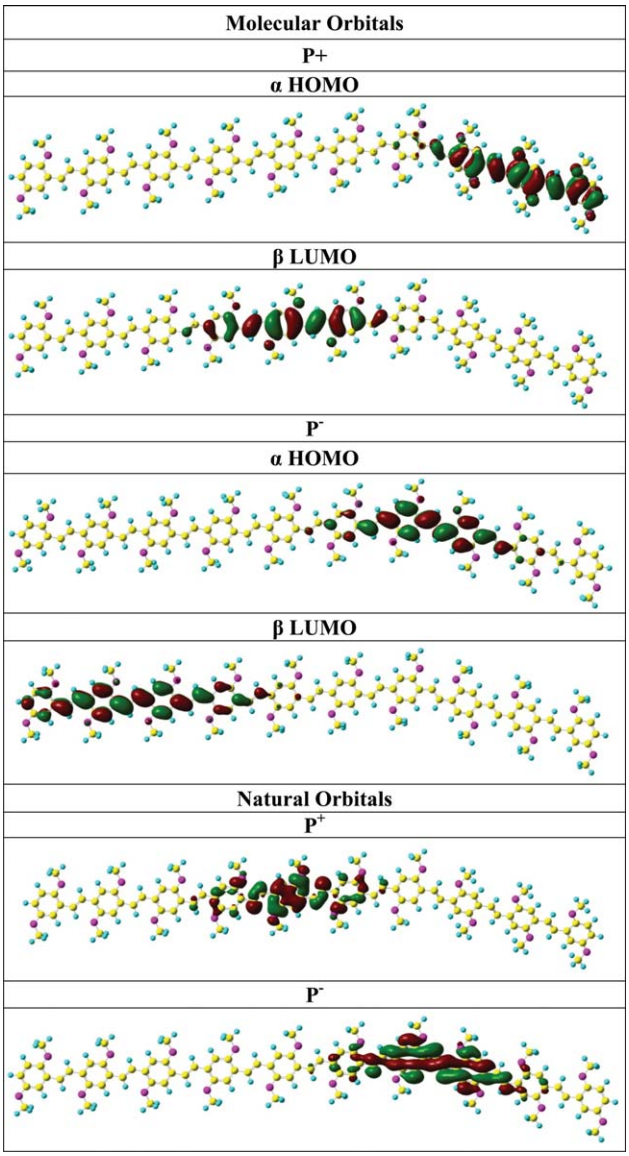

FIGURE 4 Characteristic HOMO and LUMO molecular orbitals and characteristic NOs for the singly occupied electronic levels of P^+ and P^- states in their corresponding native geometries calculated at LC-wPBE/6–31G* level in the presence of solvent for *trans*-SK (6-3) configuration of MEH-PPV oligomer.

CONCLUSIONS

In summary, we presented a detailed computational study and analysis of the energetics and spatial localization of polaronic excitations in conjugated phenylene vinylene oligomers with weak and strong conformational distortions. We observe that the particle-hole symmetry for undistorted all-*trans* MEH-PPV geometries is broken with the introduction of weak-*trans* defects. As opposed to being localized in the middle of the chain, the electron is attracted to the defect site, whereas the hole is repelled away. At the same time, both holes and electrons are repelled away from the strong defect sites of *cis* nature. The localization patterns for the polaronic excitations were observed to be invariant with respect to the position of defects along the chain. Inclusion of a polarizable dielectric medium (solvent) is found to be crucial for the self-trapping of positive and negative polarons. However, it has a different influence on the two distinct origins of localization. The polar solvent tends to increase the lattice distortion during geometry relaxation processes for P^-, whereas P^+ shows less localization than the gas phase. The solvent tends to increase the spatial confinement of the electronic wavefunction for both types of polarons although the effect is highly pronounced for P^+. This is in clear agreement with an experimental study,[27] where the electrons are reported to be more localized than the hole for MEH-PPV oligomers. On the other hand, the pristine PPV chains preserve the particle-hole symmetry even with the introduction of these defects. The *trans* isomers are observed to localize the charges in the middle, whereas the polarons are spatially kept away from the *cis*-defect positions. The solvent seems to enhance the extent of lattice and spin distortion equally for P^+ and P^- for all geometry types. The larger binding and solvation energies for P^- in comparison to P^+ in MEH-PPV than unsubstituted PPV elucidates the distinct localization patterns for holes and electrons in these oligomers.

We also found that the localized P^+ and P^- states exhibit double-well potentials for weak-*trans* distorted geometries of MEH-PPV oligomers. The energy difference between the two wells is much higher for P^- than P^+. Thus, the hole is observed to have higher drift mobilities in weak-*trans* MEH-PPV geometries than the electrons as also predicted by their observed lower reorganization energies according to Marcus hopping model.[50] Hence, this study allows us to tune the charge-transport and photophysical properties in conjugated organic materials by understanding their structure–property relationships.

ACKNOWLEDGMENTS

I. H. Nayyar, D. L. Smith, and R. L. Martin acknowledge the support from the DOE Office of Basic Energy Sciences (OBES) under Work Proposal Number 08SCPE973. S. Tretiak, A. Saxena, and E. R. Batista acknowledge the support from the US Department of Energy and Los Alamos National Laboratory (LANL) Directed Research and Development Funds. Los Alamos National Laboratory is operated by Los Alamos National Security, LLC, for the National Nuclear Security Administration of the U.S. Department of Energy under contract DE-AC52-06NA25396.

REFERENCES AND NOTES

1 A. J. Heeger, *Chem. Soc. Rev.* **2010**, *39*, 2354–2371.

2 N.-J. Lee, D.-H. Lee, D.-W. Kim, J.-H. Lee, S. H. Cho, W. S. Jeon, J. H. Kwon, M. C. Suh, *Dyes Pigments* **2012**, *95*, 221–228.

3 I. H. Campbell, D. L. Smith, S. Tretiak, R. L. Martin, C. J. Neef, J. P. Ferraris, *Phys. Rev. B* **2002**, *65*, 085210(8).

4 S. Kola, J. Sinha, H. E. Katz, *J. Polym. Sci. Part B: Polym. Phys.* **2012**, *50*, 1090–1120.

5 P. Lin, F. Yan, *Adv. Mater.* **2012**, *24*, 34–51.

6 J. Shi, Z. Chai, C. Zhong, W. Wu, J. Hua, Y. Dong, J. Qin, Q. Li, Z. Li, *Dyes Pigments* **2012**, *95*, 244–251.

7 G. Chidichimo, L. Filippelli, *Int. J. Photoenergy* **2010**, *2010*, 123534(11).

8 H. Hoppe, N. Sariciftci, *J. Mater. Res.* **2004**, *19*, 1924–1945.

9 Y. Matsuo, *Chem. Lett.* **2012**, *41*, 754–759.

10 S. Reineke, K. Walzer, K. Leo, *Phys. Rev. B* **2007**, *75*, 125328(13).

11 V. K. Thorsmølle, R. D. Averitt, J. Demsar, D. L. Smith, S. Tretiak, R. L. Martin, X. Chi, B. K. Crone, A. P. Ramirez, A. J. Taylor, *Phys. Rev. Lett.* **2009**, *102*, 017401(11).

12 M. C. Traub, G. Lakhwani, J. C. Bolinger, Vanden D. Bout, P. F. Barbara, *J. Phys. Chem. B* **2011**, *115*, 9941–9947.

13 Y. Gao, T. P. Martin, E. T. Niles, A. J. Wise, A. K. Thomas, J. K. Grey, *J. Phys. Chem. C* **2010**, *114*, 15121–15128.

14 Z. Sun, S. Stafstrom, *J. Chem. Phys.* **2012**, *136*, 244901(5).

15 L. Ge, S. Li, T. F. George, X. Sun, *Phys. Lett. A* **2008**, *372*, 3375–3379.

16 C. Bounioux, E. A. Katz, Yerushalmi-Rozen, R.*Polym. Adv. Technol.* **2012**, *23*, 1129–1140.

17 F. Labat, Le T. Bahers, I. Ciofini, C. Adamo, *Acc. Chem. Res.* **2012**, *45*, 1268–1277.

18 A. Kohler, D. A. dos Santos, D. Beljonne, Z. Shuai, J. L. Bredas, A. B. Holmes, A. Kraus, K. Mullen, R. H. Friend, *Nature* **1998**, *392*, 903–906.

19 H. Zhongjian, S. Tang, A. Ahlvers, S. I. Khondaker, A. J. Gesquiere, *Appl. Phys. Lett.* **2012**, *101*, 053308(4).

20 A. Kokil, K. Yang, J. Kumar, *J. Polym. Sci. Part B: Polym. Phys.* **2012**, *50*, 1130–1144.

21 Y. Meng, X. J. Liu, B. Di, Z. An, *J. Chem. Phys.* **2009**, *131*, 244502(5).

22 M. K. Lee, M. Segal, Z. G. Soos, J. Shinar, M. A. Baldo, *Phys. Rev. Lett.* **2005**, *94*, 137403(4).

23 K. Becker, E. Da Como, J. Feldmann, F. Scheliga, E. T. Csanyi, S. Tretiak, J. M. Lupton, *J. Phys. Chem. B* **2008**, *112*, 4859–4864.

24 G. A. Sherwood, R. Cheng, K. Chacon-Madrid, T. M. Smith, L. A. Peteanu, J. Wildeman, *J. Phys. Chem. C* **2010**, *114*, 12078–12089.

25 R. J. Magyar, S. Tretiak, Y. Gao, H. L. Wang, A. P. Shreve, *Chem. Phys. Lett.* **2005**, *401*, 149–156.

26 T. D. Nguyen, G. Hukic-Markosian, F. J. Wang, L. Wojcik, X. G. Li, E. Ehrenfreund, Z. V. Vardeny, *Nat. Mater.* **2010**, *9*, 345–352.

27 D. R. McCamey, K. J. van Schooten, W. J. Baker, S. Y. Lee, S. Y. Paik, J. M. Lupton, C. Boehme, *Phys. Rev. Lett.* **2010**, *104*, 017601(4).

28 R. Osterbacka, M. Wohlgenannt, M. Shkunov, D. Chinn, Z. V. Vardeny, *J. Chem. Phys.* **2003**, *118*, 8905–8916.

29 K. Z. Yin, L. F. Zhang, C. Lai, L. L. Zhong, S. Smith, H. Fong, Z. T. Zhu, *J. Mater. Chem.* **2011**, *21*, 444–448.

30 I. H. Nayyar, E. R. Batista, S. Tretiak, A. Saxena, D. L. Smith, R. L. Martin, *J. Phys. Chem. Lett.* **2011**, *2*, 566–571.

31 I. H. Nayyar, E. R. Batista, S. Tretiak, A. Saxena, D. L. Smith, R. L. Martin, *J. Chem. Theory Comput.* **2013**, *9*, 1144–1154.

32 C. Melzer, E. J. Koop, V. D. Mihailetchi, P. W. M. Blom, *Adv. Funct. Mater.* **2004**, *14*, 865–870.

33 J. E. Norton, J.-L. Bredas, *J. Am. Chem. Soc.* **2008**, *130*, 12377–12384.

34 P. Yang, E. R. Batista, S. Tretiak, A. Saxena, R. L. Martin, D. L. Smith, *Phys. Rev. B* **2007**, *76*, 241201(4).

35 S. Kilina, E. R. Batista, P. Yang, S. Tretiak, A. Saxena, R. L. Martin, D. L. Smith, *ACS Nano* **2008**, *2*, 1381–1388.

36 Y. Li, H. Xu, L. Wu, F. He, F. Shen, L. Liu, B. Yang, Y. Ma, *J. Polym. Sci. Part B: Polym. Phys.* **2008**, *46*, 1105–1113.

37 E. J. Harbron, D. H. Hadley, M. R. Imm, *J. Photochem. Photobiol. A: Chem.* **2007**, *186*, 151–157.

38 A. F. Grimes, S. E. Call, E. J. Harbron, D. S. English, *J. Phys. Chem. C* **2007**, *111*, 14257–14265.

39 S. M. Lewis, E. J. Harbron, *J. Phys. Chem. C* **2007**, *111*, 4425–4430.

40 S. Son, A. Dodabalapur, A. J. Lovinger, M. E. Galvin, *Science* **1995**, *269*, 376–378.

41 D. Liu, S. Yin, H. Xu, X. Liu, G. Sun, Z. Xie, B. Yang, Y. Ma, *Chem. Phys.* **2011**, *388*, 69–77.

42 S. Tretiak, K. Igumenshchev, V. Chernyak, *Phys. Rev. B* **2005**, *71*, 033201.

43 K. I. Igumenshchev, S. Tretiak, V. Y. Chernyak, *J. Chem. Phys.* **2007**, *127*, 114902.

44 R. J. Magyar, S. Tretiak, *J. Chem. Theory Comput.* **2007**, *3*, 976–987.

45 M. J. Frisch, G. W. Trucks, H. B. Schlegel, G. E. Scuseria, M. A. Robb, J. R. Cheeseman, G. Scalmani, V. Barone, B. Mennucci, G. A. Petersson, H. Nakatsuji, M. Caricato, X. Li, H. P. Hratchian, A. F. Izmaylov, J. Bloino, G. Zheng, J. L. Sonnenberg, M. Hada, M. Ehara, K. Toyota, R. Fukuda, J. Hasegawa, M. Ishida, T. Nakajima, Y. Honda, O. Kitao, H. Nakai, T. Vreven, J. A. Montgomery, Jr., J. E. Peralta, F. Ogliaro, M. Bearpark, J. J. Heyd, E. Brothers, K. N. Kudin, V. N. Staroverov, R. Kobayashi, J. Normand, K. Raghavachari, A. Rendell, J. C. Burant, S. S. Iyengar, J. Tomasi, M. Cossi, N. Rega, N. J. Millam, M. Klene, J. E. Knox, J. B. Cross, V. Bakken, C. Adamo, J. Jaramillo, R. Gomperts, R. E. Stratmann, O. Yazyev, A. J. Austin, R. Cammi, C. Pomelli, J. W. Ochterski, R. L. Martin, K. Morokuma, V. G. Zakrzewski, G. A. Voth, P. Salvador, J. J. Dannenberg, S. Dapprich, A. D. Daniels, Ö. Farkas, J. B. Foresman, J. V. Ortiz, J. Cioslowski, D. J. Fox, Gaussian-09, Revision A.1, Gaussian Inc., Wallingford CT, **2009**.

46 S. Tretiak, A. Saxena, R. L. Martin, A. R. Bishop, *Phys. Rev. Lett.* **2002**, *89*, 097402(4).

47 S. R. Marder, L. T. Cheng, B. G. Tiemann, A. C. Friedli, M. Blancharddesce, J. W. Perry, J. Skindhoj, *Science* **1994**, *263*, 511–514.

48 V. M. Geskin, J. Cornil, J. L. Bredas, *Chem. Phys. Lett.* **2005**, *403*, 228–231.

49 V. M. Geskin, F. C. Grozema, L. D. A. Siebbeles, D. Beljonne, J. L. Bredas, J. Cornil, *J. Phys. Chem. B* **2005**, *109*, 20237–20243.

50 R. A. Marcus, *Rev. Mod. Phys.* **1993**, *65*, 599–610.